Decay of a Diffractively Excited Cluster and the Exclusive Components for Inclusive Reactions

C. S. Lam*
Department of Applied Mathematics and Theoretical Physics, University of Cambridge, Cambridge, England
(Received 2 June 1972)

In most of the recent diffractive-model calculations for inclusive reactions, the diffractively excited cluster is assumed to decay isotropically and no correlation is assumed to exist among the decay products. The importance of including at least the correlations due to energy-momentum conservation is emphasized, and the consequences for such an inclusion are analyzed. Very definite predictions are obtained for the multiplicity and momentum distributions coming from such a decay, and these should be compared with experiments in order to gain an understanding into the internal structure of excited hadrons.

I. INTRODUCTION

There are two main mechanisms in the diffractive model[1] for particle productions. One or both of the incoming particles are assumed to be diffractively excited into fireballs, before they subsequently decay into a cluster of observed particles. Different authors[1-4] assume different fireball production cross sections, but all of them assume that the fireballs decay in a spherically symmetric manner with minimal amount of correlations. In other words, if energy-momentum conservation is ignored, then the particle decay is described as a product of single-particle decay distributions, each of which is spherically symmetrical in the rest frame of the fireball. It is the aim of this paper to analyze the consequences of this hypothesis and how they can be tested experimentally.

Actually, in most of the previous calculations,[1-3,5-7] technical difficulties prevented the proper inclusion of energy-momentum conservation[8] so that the hypothesis above was not even obeyed to the letter. Momentum conservation was ignored altogether, and energy conservation was taken into account only approximately by assuming a relation between the fireball mass M_1 and the number of pions n it decays into. This mutilated hypothesis ignores one of nature's most fundamental conservation laws, and is certainly not strictly correct. Various correlation effects due to energy-momentum conservation are thus washed out. For the single-particle inclusive spectrum, interesting correlations between the transverse and the longitudinal momenta[9] are thereby lost. For a two-particle inclusive spectrum, this produces a peak in y_1 shifting towards the right when y_2 is increased,[7] where y_1 and y_2 are the rapidities of the detected particles. Experimentally the peak moves the other way, presumably due at least in part to energy-momentum conservation. From a different point of view, Białas *et al.*[10] have also pointed out the importance of this conservation law. Moreover, energy conservation taken into account in this approximate manner makes n a continuous variable since M_1 is continuous. This has several immediate drawbacks, the most obvious of which is that this prevents us from calculating cross sections for exclusive reactions, where the number of pions always appears as an integer. Even in inclusive reactions, where the number of pions is summed and in this approximation the sum is replaced by an integral, it is not clear whether the lower limit of the integral should be taken to be 1, or 0.5 according to the trapezoidal rule, or to correspond to the threshold mass M_1^0 of the fireball. Since the single-particle spectrum is known[2,3] to be very sensitive to this lower limit, this matter clearly has to be decided. When the two-particle spectrum is calculated, this dilemma becomes much more serious because there a factor $n(n-1)$ appears. If n is between 0 and 1, as is possible if the last two alternatives of choosing its lower limit are adopted, then this factor, as well as the cross section, can actually become negative. One application of our analysis of the unmutilated hypothesis, with energy-momentum conservation properly taken into account, is to provide a method and explicit formulas by which the drawbacks mentioned in this paragraph may be avoided.

In Sec. II and in the Appendix, this decay hypothesis is formulated mathematically, and an approximate method is developed whereby consequences of this hypothesis may be obtained. These consequences in explicit mathematical formulas are discussed in Sec. III together with their

qualitative physical implications. Finally, how these consequences may be tested experimentally are discussed in Sec. IV.

II. CONSEQUENCE OF THE DECAY HYPOTHESIS

Let M_1 be the mass of a diffractively excited cluster, decaying subsequently into n particles with momenta $\vec{k}_i$ $(1 \leq i \leq n)$. We assume, in the spirit of Refs. 1–4 and 9, that the decay distribution is given by a product of n single-particle functions $g_i(k_i)$ $(k_i \equiv \sqrt{\vec{k}_i^{\,2}})$, if energy-momentum conservation is ignored. Energy-momentum conservation then comes in to determine n and all observed correlations.

In other words, we assume that the joint probability density for finding n particles with momenta $\vec{k}_i$ $(1 \leq i \leq n)$ in the cluster is given by

$$P_0(\vec{k}_1, \ldots, \vec{k}_n) = c \prod_{i=1}^{n} g_i(k_i) \delta^4\Big(\sum_{i=1}^{n} k_i^\mu - K^\mu\Big), \tag{1}$$

where

$$k_i^\mu = ((k_i^2 + m_i^2)^{1/2}, \vec{k}_i)$$

and

$$K^\mu = (M_1, \vec{0}),$$

$$\int g_i(\vec{k})\, d^3k = 1. \tag{2}$$

Here c is a constant independent of n and $\vec{k}_i$. The probability density for finding a total of n particles in the cluster, with the first m of them occupying momenta $\vec{k}_1, \ldots, \vec{k}_m$ and the remaining $n-m$ of them having any momentum, is obtained by integrating (1) $n-m$ times. This gives

$$P_{n-m}(\vec{k}_1, \ldots, \vec{k}_m) = c \prod_{i=1}^{m} g_i(k_i) \int d^3k_{m+1} \cdots d^3k_n \sum_{j=m+1}^{n} g_j(k_j) \delta^4\Big(\sum_{i=1}^{n} k_i^\mu - K^\mu\Big). \tag{3}$$

In particular, the probability for finding n particles with any momentum is

$$P_n = c \int \prod_{i=1}^{n} d^3k_i\, g_i(k_i) \delta^4\Big(\sum_{i=1}^{n} k_i^\mu - K^\mu\Big), \tag{4}$$

from which c can be determined by the condition

$$\sum_n P_n = 1. \tag{5}$$

The sum in (5) is carried out over all n consistent with the conservation laws. For example, if the cluster is an excited pion cluster, and n is the number of pions, then n has to be an odd number not less than 3.

The integrals that have to be carried out are all of the form

$$\mathcal{G}_n(p) = \int \prod_{i=1}^{N} d^3k_i\, g_i(k_i) \delta^4\Big(\sum_{j=1}^{N} k_j^\mu - p^\mu\Big). \tag{6}$$

If $N=1$, the integral can easily be performed:

$$\mathcal{G}_1(p) = g_1((\vec{p}^{\,2})^{1/2})\, \delta((\vec{p}^{\,2} + m_1^2)^{1/2} - p^0). \tag{7}$$

If $N=2$, sometimes the integral can still be done. For example, if $g_i(k) = (\alpha/\pi)^{3/2} \exp(-\alpha_i k^2)$, and $\vec{p} = \vec{0}$, then

$$\mathcal{G}_2(p) = 4\pi(\alpha_1\alpha_2/\pi^2)^{3/2} \exp[-(\alpha_1+\alpha_2)k^2] k k_1^0 k_2^0/p^0, \tag{8}$$

where

$$k = \lambda^{1/2}((p^0)^2, m_1^2, m_2^2)/2p^0,$$

$$\lambda(a, b, c) \equiv (a+b-c)^2 - 4ab \tag{9}$$

$$k_1^0 = ((p^0)^2 + m_1^2 - m_2^2)/2p^0,$$

$$k_2^0 = ((p^0)^2 + m_2^2 - m_1^2)/2p^0.$$

For $N \geq 3$, the integral in (6) usually cannot be done analytically. The rest of this section is devoted to finding an approximate method whereby such an integral may be carried out.

Equation (6) can be written as

$$\mathcal{G}_N(p) = (2\pi)^{-4} \int e^{-ip\cdot x} \prod_{i=1}^{N} \tilde{g}_i(x) d^4x, \tag{10}$$

where

$$p \cdot x = -p^0 x^0 + \vec{p} \cdot \vec{x},$$

$$\tilde{g}_i(x) = \int e^{ik\cdot x} g_i(k) d^3k. \tag{11}$$

One method of treating (10) that has become rather popular[11] is that of Khinchin.[12] This makes use of the fact that $\tilde{g}_i(x)$ is analytic in x, owing to the damping of $g_i(k)$ for large k. Therefore the contour in x space in Eq. (10) can be pushed into the complex x space. $\ln\prod_{i=1}^{N} \tilde{g}_i(x)$ is then expanded into a power series about a point $x = -i\xi$. The integral (10) can then be done term by term, and the result is an expansion in N^{-1}. The point ξ is chosen so that this expansion in N^{-1} converges fastest in some sense. Unfortunately this elegant method is unsuitable for the present analysis, for two reasons. First, it is very difficult in actual calculations because it involves the determination of the four-vector ξ^μ. Second, a large portion of the physics is buried in this vector ξ^μ so that even if a numerical determination of ξ^μ is feasible,

its physical content is far from being transparent. Therefore, we will adopt an alternative method, which results in an expansion in N^{-1} not converging as fast as the Khinchin method. This simply means that more terms have to be included. However, this method has several advantages: No determination of ξ^μ is necessary, the physical content of the final formula is transparent, and a systematic graphical rule very similar to the Feynman rules can be developed for this expansion

The present method consists of an expansion of $\ln\prod_{i=1}^{N}\bar{g}_i(x)$ about $x=0$. This is possible because $\bar{g}_i(0)=1$, owing to (2). Suppose the expansion is

$$\ln\prod_{i=1}^{N}\bar{g}_i(x)=\sum_{l=1}^{\infty}\frac{i^l}{l!}A^{(l)}_{\mu_1\cdots\mu_l}x^{\mu_1}\cdots x^{\mu_l}\,. \tag{12}$$

Substituting (12) into (10), we obtain

$$\mathcal{G}_N(p)=(2\pi)^{-4}\int\exp[-i\bar{p}\cdot x-\tfrac{1}{2}x^\alpha A^{(2)}_{\alpha\beta}x^\beta]H(x)d^4x\,, \tag{13}$$

where

$$\bar{p}=p-A^{(1)}\,, \tag{14}$$

$$H(x)=\exp\left(\sum_{l=3}^{\infty}\frac{i^l}{l!}A^{(l)}_{\mu_1\cdots\mu_l}x^{\mu_1}\cdots x^{\mu_l}\right). \tag{15}$$

Expanding H in power series of x, the integral in (13) can be evaluated term by term. The result is

$$\mathcal{G}_N(p)=(2\pi)^{-2}(\det A^{(2)})^{-1/2}H\left(i\frac{\partial}{\partial\bar{p}}\right)\times\exp(-\tfrac{1}{2}\bar{p}_\alpha B^{\alpha\beta}\bar{p}_\beta)\,, \tag{16}$$

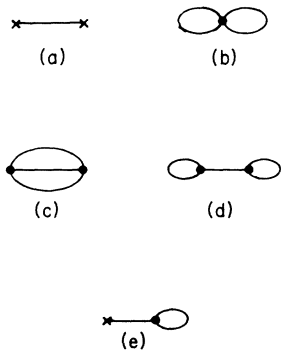

FIG. 1. Diagrams (a)–(e) in the first column of Table I.

where

$$B^{\alpha\beta}A^{(2)}_{\beta\gamma}=\delta^\alpha{}_\gamma. \tag{17}$$

The expression in (16) resembles closely what we would get in deriving the Feynman rules using the external-sources technique.[13] In fact, similar rules can be derived for (16). The expression $(2\pi)^2(\det A^{(2)})^{1/2}\mathcal{G}_N(p)$ is given by a sum of Feynman-like diagrams, some of which are listed in Table I. Each propagator (——) takes a factor $-B^{\alpha\beta}$, each external source (×) takes a factor $\bar{p}$, and each l-prong vertex corresponds to a factor $(-1)^l A^{(l)}_{\mu_1\cdots\mu_l}$. Instead of integrating over all internal momenta, as in usual Feynman rules, we merely have to sum over all indices. Thus each diagram can be computed with only algebra. No integrations are involved. Finally, just as in Feynman diagrams, an extra symmetry factor S^{-1} must be multiplied into the whole expression, where S is the number of ways the diagram may be permuted into itself without breaking any of the lines. For an illustration of S, see Table I.

Just as in usual Feynman diagrams, there are connected and disconnected diagrams, and the sum of all diagrams is simply the exponential of the sum of all connected diagrams.

We therefore obtain finally the expression

$$\mathcal{G}_N(p)=(2\pi)^{-2}(\det A^{(2)})^{-1/2}\exp(\Sigma_c)\,, \tag{18}$$

where Σ_c is the sum of all connected diagrams.

The expansion of Σ_c in terms of various connected diagrams can be grouped into an expansion in N^{-1}. To do this, first notice that it follows from (12) that

$$A^{(l)}_{\mu_1\cdots\mu_l}=\sum_{i=1}^{N}(-i)^l\frac{\partial^l}{\partial x^{\mu_1}\cdots\partial x^{\mu_l}}\ln\bar{g}_i(x)\,. \tag{19}$$

Therefore each $A^{(l)}$ is of order N, and the propagator B is of order N^{-1}. Consequently a diagram which consists of G propagators, V_l l-prong vertices, and E external sources behaves like N^{-D},

TABLE I. Connected diagrams of order N^{-1}. The diagrams of the first column are found in Fig. 1.

Diagram (See Fig. 1)	S	Expression
(a)	2	$-\frac{1}{2}\bar{p}_\alpha B^{\alpha\beta}\bar{p}_\beta\equiv-(\bar{p}^0)^2Z_4-\vec{\mathbf{p}}^2Z_5$
(b)	$(2)^3$	$\frac{1}{8}A^{(4)}_{\alpha\beta\gamma\delta}B^{\alpha\beta}B^{\gamma\delta}\equiv Z_0$
(c)	2(3!)	$-\frac{1}{12}A^{(3)}_{\alpha\beta\gamma}A^{(3)}_{\lambda\mu\nu}B^{\alpha\lambda}B^{\beta\mu}B^{\gamma\nu}\equiv-Z_1$
(d)	$(2)^3$	$-\frac{1}{8}A^{(3)}_{\alpha\beta\gamma}A^{(3)}_{\lambda\mu\nu}B^{\alpha\beta}B^{\lambda\mu}B^{\gamma\nu}\equiv-Z_2$
(e)	2	$-\frac{1}{2}A^{(3)}_{\alpha\beta\gamma}B^{\alpha\beta}B^{\gamma\delta}\bar{p}_\delta\equiv\bar{p}^0Z_3$

where

$$D = G - \sum_{l=3}^{\infty} V_l . \tag{20}$$

On the other hand, topologically we must have

$$E + \sum_{l=3}^{\infty} l V_l = 2G . \tag{21}$$

Combining (20) and (21), we get

$$D = \tfrac{1}{2}\left(\sum_{l=3}^{\infty} (l-2) V_l + E\right). \tag{22}$$

This leads to $D \geq 1$. The term $D = 1$ is comprised of diagrams exhibited in Table I. If we should want more accurate expressions we can always include higher-order diagrams. In the following discussions, we will confine ourselves to terms in Table I only.

To obtain an explicit formula for $\mathcal{G}_N(p)$, we have to substitute the expressions in Table I into Eq. (18), and express $A^{(l)}$ in terms of the various moments of distributions $g_i(k)$. The computation is straightforward, but rather lengthy. It is carried out in the Appendix. However, we can already see from Table I that the result is of the form

$$\mathcal{G}_N(p) = (2\pi)^{-2} (\det A^{(2)})^{-1/2} \times \exp[Z_6 + \bar{p}^0 Z_3 - (\bar{p}^0)^2 Z_4 - \vec{\mathbf{p}}^2 Z_5], \tag{23}$$

where

$$Z_6 = Z_0 - Z_1 - Z_2 . \tag{24}$$

The detailed expressions for Z_i as well as $\det A^{(2)}$ are given in the Appendix. Suffice it to note here that each Z_i is of order N^{-1}, and $\det A^{(2)}$ is of order N^4. Further discussions of this formula will be postponed to the next section.

It is well known that the transverse momenta of the particles emerging from a reaction are bounded, and are roughly constant depending only on what particle we measure. It is therefore more interesting to study the longitudinal momentum variations, which change from reaction to reaction. For this latter study, it is sometimes useful to treat the transverse momentum of each particle as strictly a constant, and concentrate only on its longitudinal momentum distributions. This was, for example, done in Ref. 2. When this is done, the four-dimensional (4D) formulas developed above have to be modified into the corresponding two-dimensional (2D) formulas in the following way.

All four-dimensional vectors and integrations are changed into two-dimensional vectors and integrations. Similarly three-dimensional integrations are changed into one-dimensional integrations. The energy-momentum conservation δ function is now two-dimensional, depicting energy and longitudinal momentum conservation. The mass m_i of a particle should be replaced by $m_{i\perp} = (m_i^2 + k_{i\perp}^2)^{1/2}$, with the perpendicular momentum $k_{i\perp}$ taken into account. The result is to change Eqs. (7) and (8) into

$$\mathcal{G}_1(p) = g_1(p)\delta((p^2 + m_{1\perp}^2)^{1/2} - p^0), \tag{7'}$$

$$\mathcal{G}_2(p) = (\alpha_1\alpha_2/\pi)^{1/2} \exp[-(\alpha_1 + \alpha_2)k^2] k_1^0 k_2^0 / k p^0 , \tag{8'}$$

with k, k_1^0, k_2^0 defined as in (9), except with m_i replaced by $m_{i\perp}$. Equations (18) and (23) are modified to become

$$\mathcal{G}_N(p) = (2\pi)^{-1} (\det A^{(2)})^{-1/2} \exp(\Sigma_c) \tag{18'}$$

$$= (2\pi)^{-1} (\det A^{(2)})^{-1/2} \exp[Z_6 + \bar{p}^0 Z_3 - (\bar{p}^0)^2 Z_4 - \vec{\mathbf{p}}^2 Z_5] + O(N^{-2}), \tag{23'}$$

where $A^{(2)}$ is now a 2×2 matrix. The detailed expressions for Z_i for this 2D case can again be found in the Appendix.

III. DECAY OF A FIREBALL

We will discuss in this section the result of Sec. II. Only the 4D formulas are considered. The 2D formulas behave in much the same way.

From Eqs. (14), (23), (A4), and (A5), we get

$$\mathcal{G}_N(p) = (2\pi)^{-2} (\det A^{(2)})^{-1/2} \times \exp[Z_6 + \bar{p}^0 Z_3 - (\bar{p}^0)^2 Z_4 - \vec{\mathbf{p}}^2 Z_5], \tag{25}$$

where

$$\bar{p}^0 = p^0 - \sum_{i=1}^{N} \langle k^0 \rangle_i .$$

Notice from Eq. (A11) that $Z_4 > 0$ and $Z_5 > 0$. The various probability distributions are obtained by comparing (1)–(5) with (6). Thus

$$P_N = c\mathcal{G}_N(K), \tag{26}$$

$$P_N(\vec{\mathbf{k}}_1) = c\, g_1(k_1)\mathcal{G}_N(K - k_1), \tag{27}$$

$$P_N(\vec{\mathbf{k}}_1, \vec{\mathbf{k}}_2) = c\, g_1(k_1) g_2(k_2)\mathcal{G}_N(K - k_1 - k_2), \tag{28}$$

and so on

Consider first Eq. (26). Here $\bar{p}^0 = M_1 - \sum_{i=1}^{N} \langle k^0 \rangle_i \equiv \delta M_1$ measures how much the actual available energy deviates from the mean total energy if there is no energy conservation. Remembering that $\vec{\mathbf{p}} = 0$, the exponential in Eq. (25) describes a prob-

ability distribution which reaches a maximum at

$$M_1 - \sum_{i=1}^{N} \langle k^0 \rangle_i = \frac{Z_3}{2Z_4} \tag{29}$$

and falls to zero like a Gaussian as $|\vec{p}^0|$ becomes large. Considered as a function of N for fixed M_1, it therefore peaks at a point N_0 determined by (29) and falls to zero on both sides of it with a width of order of $N_0^{1/2}$. The factor $(\det A^{(2)})^{-1/2}$ gives rise to a quantitative adjustment, but the qualitative behavior for P_N is still the same. Note that Z_3 and Z_4 are both of order N^{-1}; hence the right-hand side of (29) is of order 1. A numerical calculation indicates that this right-hand side is a small number (see Fig. 2), and thus the peak is approximately determined by

$$\delta M_1 = 0 \tag{30}$$

as was assumed in Refs. 1–3. However, in Refs. 1–3, the width of the N distribution is assumed to be constant (zero), whereas we see here that the width grows like $N_0^{1/2}$. This spreading has the effect in changing the single-particle spectrum of the inclusive reactions for small c.m. momenta. Incidentally, the result of zero width will be recovered by letting $Z_4 \to \infty$.

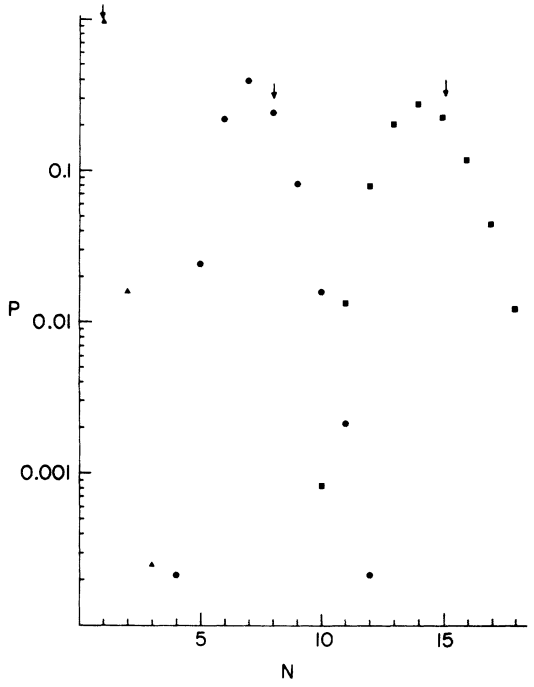

FIG. 2. Probability distribution P as a function of the number of pions N. The cluster masses M_1 are ▲ = 1.5 GeV, ● = 4.5 GeV, and ■ = 7.5 GeV. The arrows indicate positions determined by Eq. (30). The parameters used are α(proton) = 4.0 $(\mathrm{GeV}/c)^{-2}$ and α(pion) = 8.2 $(\mathrm{GeV}/c)^{-2}$.

To illustrate the behavior of P_N, a numerical computation has been carried out for the proton cluster using Eq. (A1). The numerical values adopted are those close to the experimental values,[2,9] namely, $\alpha(\text{proton}) = 4.0\ (\mathrm{GeV}/c)^{-2}$ and $\alpha(\text{pion}) = 8.2\ (\mathrm{GeV}/c)^{-2}$. The results for three values of M_1 are shown in Fig. 2. The arrows on top of the diagram indicate positions determined from (30) for the three masses. The points drawn have their overall normalizations already adjusted according to Eq. (5). Before such an adjustment, the values for $g_2(K)$ (corresponding to one pion being emitted) determined from (25) are 0.96 and 0.22×10^{-37}, respectively, for $M_1 = 1.5$ and 4.5 GeV. The exact values determined from (8) are 0.997 and 0.597×10^{-22}, respectively. It is gratifying to note that even for $N=2$, a very good approximation (4% for $M_1 = 1.5$ GeV) is obtained where the $N=2$ term is important ($M_1 = 1.5$ GeV). The approximation for such a low N becomes very bad for large M_1(e.g., $M_1 = 4.5$ GeV), but there the value is so small that it does not matter anyway.

We now come to the single-particle distribution (27). If $Z_4 \to \infty$, we obtain the product of a δ function located at an N value determined by

$$M_1 - \sum_{i=1}^{N} \langle k^0 \rangle_i = (k_1^2 + m_1^2)^{1/2} \tag{31}$$

and the factor $g_1(k_2)\exp(-Z_5 k_1^2)$. This is the result obtained in Ref. 9, where momentum conservation is taken into account exactly but energy conservation is included only to the extent of (31). The extra factor $\exp(-Z_5 \vec{k}_1^{\,2})$, which becomes unity when $N \to \infty$, comes from the momentum cutoff factor $g_i(k_i)$ of the recoiling particles ($i \neq 1$). The recoil for each particle becomes negligible when $N \to \infty$, which is why the factor becomes one in that limit.

If Z_4 remains what it should be, we see from (25) and (27) that the δ function has to be broadened into the function $g_N(K_1)$, where

$$K_1^{\mu} = \left(M_1 - (k_1^2 + m_1^2)^{1/2} - \sum_{i=1}^{N} \langle k^0 \rangle_i , 0 \right) .$$

The dependence on k_1 in this factor, which comes essentially from energy conservation, is reflected in an interesting way in the over-all k_1 dependence. According to (25), $g_N(K_1)$ reaches a maximum at

$$M_1 - \sum_{i=1}^{N} \langle k^0 \rangle_i - (k_1^2 + m_1^2)^{1/2} = Z_3/2Z_4 . \tag{32}$$

Thus if M_1 and N were fixed at a value so that K_1^0 lies to the right of this peak, an increase in k_1 would decrease K_1^0, so that $g_N(K_1)$ would increase until we get past the peak. As a result, the over-

all k_1 dependence in $P_N(\vec{k}_1)$ might increase towards a maximum before it subsequently decreases, as is the case in curve 1 of Fig. 3. If we start on the other side of the peak, then $g_N(K_1)$ decreases, and $P_N(\vec{k}_1)$ would decrease even faster than that given by $g_1(k_1)\exp(-Z_5 k_1^2)$. Such effects may also be seen by writing (25) and (27) in the form

$$P_N(\vec{k}_1) = P_N \exp[\rho(k_1^2+m_1^2)^{1/2} - (Z_4+Z_5)k_1^2 - Z_4 m_1^2]g_1(k_1),$$
$$\rho = -Z_3 + 2Z_4\delta M_1 . \tag{33}$$

As an illustration, the k_1 dependence is plotted in Figs. 3 and 4 using the same parameters as in Fig. 2. The normalization of each curve is arbitrary. The cluster mass used is 4.5 GeV throughout. In both Figs. 3 and 4, curve 1 refers to $\exp(-\alpha k^2)$, and curves 2, 3, 4, and 5 refer to cases where the total number of pions is respectively 4, 6, 8, or 9.

Finally, the behavior of the two-particle distribution functions (28) can be understood in much the same way. In addition to the uncorrelated distribution function $g_1(k_1)g_2(k_2)$, we have the extra factor g_N given by (25), with

$$\bar{p}^0 = \delta M_1 - (k_1^2+m_1^2)^{1/2} - (k_2^2+m_2^2)^{1/2},$$
$$\vec{p} = \vec{k}_1 + \vec{k}_2 . \tag{34}$$

For example, if M_1, N, k_1, and k_2 are fixed, then the only change in (28) comes from the change of the $Z_5\vec{p}^2$ term, when the relative orientations of $\vec{k}_1$ and $\vec{k}_2$ are varied. Clearly from (34), opposite orientations of these two vectors are most favored, a fact that is to be expected from momentum conservation alone. Other more complicated multiparticle correlation effects can also be analyzed in the same way.

IV. ANALYSES OF EXCLUSIVE REACTIONS

Most of the data presently available are below 30 GeV/c and possess a large nondiffractive component for most of their exclusive channels. The diffractive model for inclusive reactions at these energies is of course based on the fact that inclusive reactions seem to reach approximate limiting[14] at fairly low energy, without attempting to explain why the fact is so. To test the detailed consequences of the decay hypothesis obtained in the previous section, we must wait for data from the present generation of high-energy machines.

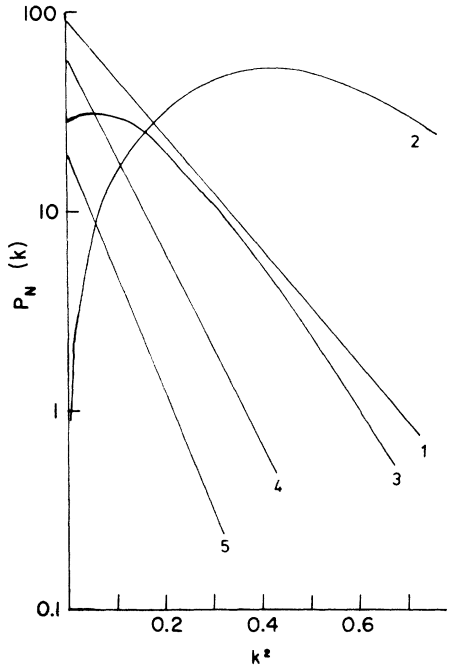

FIG. 3. Pion momentum distribution $P_N(k)$ with arbitrary normalizations. The proton cluster mass used for this illustration is 4.5 GeV. Curve 1 represents $\exp(-8.2k^2)$. The total number of pions in curves 2, 3, 4, 5 is respectively 4, 6, 8, 9. All momentum units are in GeV/c.

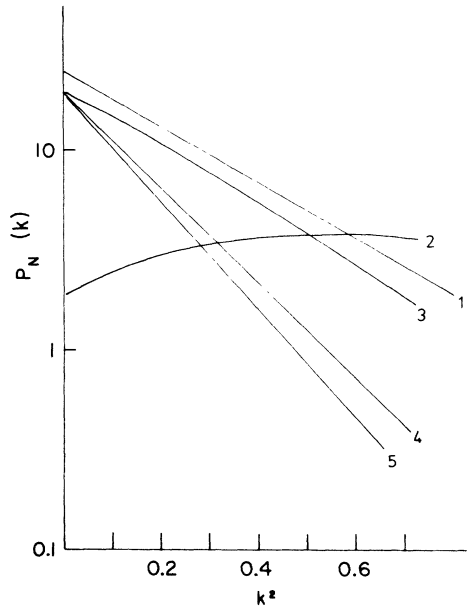

FIG. 4. Proton momentum distribution $P_N(k)$ with arbitrary normalizations. The proton cluster mass used for this illustration is 4.5 GeV. Curve 1 represents $\exp(-4.0k^2)$. The total number of pions in curves 2, 3, 4, 5 is respectively 4, 6, 8, 9. All momentum units are in GeV/c.

If the exclusive events at these high energies are mainly diffractive, then we can test the hypothesis by first grouping the events according to their fireball mass M_1, which is the invariant mass of all the particles in the forward hemisphere in the c.m. system. We can then analyze the multiplicity distributions, single-particle momentum distributions, two-particle momentum distributions, etc., and compare them with the predictions discussed in Sec. III.

The only free parameters in the formulas in Sec. III are the various moments of $g_i(k_i)$. By looking at the transverse-momentum distributions, a fair idea of the shape of $g_i(k_i)$ could be obtained. Thus, for example, we may start from moments of $g_i(k_i)$ computed that way and see how well the various predictions are fulfilled. If necessary, a fit may also be attempted by varying these moments.

Even if neutral particles go undetected in an experiment, the predictions may still be checked with one additional assumption, one that is used very frequently. (For example, this assumption leads to[2,9] correct relative normalizations and shapes between $p+p\to\pi^+ +$ anything and $p+p\to\pi^- +$ anything.) This consists of assuming that in a neutral system of pions, there are one third each of π^+, π^0, and π^-. This is to say that the probability for creating a $\pi^+\pi^-$ pair, or a pair of π^0, is $\frac{1}{2}$ for each. A neutral system of $2n$ pions therefore has a probability $(\frac{1}{2})^n$ of having no neutral pions, and a neutral system of $2n+1$ pions has probability $(\frac{1}{2})^n$ of producing n changed pairs and one neutral pion. When this factor is incorporated into the probability distributions in Eqs. (26)–(28), corresponding formulas for 4c and 1c events may be obtained. Comparison with experiments can then be made.

When events are grouped in this way, according to the fireball mass M_1, we may also decide which of the several[1-4] production mechanisms are correct. Another thing that can be done is to calculate the exclusive components for inclusive reactions and compare them with experiments. For this we need to know the production mechanism and to integrate over M_1. It is therefore not as clean a test unless we can be sure that the production mechanism is correct.

The predictions of the previous section depend only on the absence of any decay correlation other than that of energy-momentum conservation. This is clearly the simplest kind of internal structure we can assume for a diffractively excited cluster. Should large deviations from these predictions be seen, important nontrivial structures are probably present inside the cluster, and it will be very interesting to discover what they are.

ACKNOWLEDGMENTS

The hospitality of Professor J. C. Polkinghorne and other members of DAMTP is gratefully acknowledged.

APPENDIX

In this appendix we give explicit expressions for $A^{(l)}$ and Z_i [Table I and Eqs. (12), (23), and (23′)] in terms of the moments of $g_i(k)$. Both the 4D and the 2D formulas are considered. Explicit formulas are also given for the particular cases when

$$g_i(k)=(\alpha_i/\pi)^{3/2}\exp(-\alpha_i\vec{k}^2) \tag{A1}$$

or

$$g_i(k)=(\alpha_i/\pi)^{1/2}\exp(-\alpha_i k^2)\,. \tag{A2}$$

If we expand $\bar{g}_i(x)$ in the following way:

$$\bar{g}_i(x)=1+\sum_{l=1}^{\infty}\frac{i^l}{l!}\,a^{(l,i)}_{\mu_1\cdots\mu_l}x^{\mu_1}\cdots x^{\mu_l}\,, \tag{A3}$$

then

$$a^{(l,i)}_{\mu_1\cdots\mu_l}=\langle k_{\mu_1}\cdots k_{\mu_l}\rangle_i=\int g_i(k)\,d^M k\,k_{\mu_1}\cdots k_{\mu_l}\,, \tag{A4}$$

where $M=3$ and 1 for 4D and 2D cases, respectively. Comparing (12) and (A4), we obtain

$$A^{(1)}_{\alpha}=\sum_i a^{(1,i)}_{\alpha}\,,$$

$$A^{(2)}_{\alpha\beta}=\sum_i[a^{(2,i)}_{\alpha\beta}-a^{(1,i)}_{\alpha}a^{(1,i)}_{\beta}]\,,$$

$$A^{(3)}_{\alpha\beta\gamma} = \sum_i \{a^{(3,i)}_{\alpha\beta\gamma} - [a^{(1,i)}_{\alpha} a^{(2,i)}_{\beta\gamma} + a^{(1,i)}_{\beta} a^{(2,i)}_{\alpha\gamma} + a^{(1,i)}_{\gamma} a^{(2,i)}_{\alpha\beta}] + 2a^{(1,i)}_{\alpha} a^{(1,i)}_{\beta} a^{(1,i)}_{\gamma}\}, \tag{A5}$$

$$\begin{aligned} A^{(4)}_{\alpha\beta\gamma\delta} = \sum_i \{ & a^{(4,i)}_{\alpha\beta\gamma\delta} - [a^{(2,i)}_{\alpha\beta} a^{(2,i)}_{\gamma\delta} + a^{(2,i)}_{\alpha\gamma} a^{(2,i)}_{\beta\delta} + a^{(2,i)}_{\alpha\delta} a^{(2,i)}_{\beta\gamma}] - [a^{(1,i)}_{\alpha} a^{(3,i)}_{\beta\gamma\delta} + a^{(1,i)}_{\beta} a^{(3,i)}_{\alpha\gamma\delta} + a^{(1,i)}_{\gamma} a^{(3,i)}_{\alpha\beta\delta} + a^{(1,i)}_{\delta} a^{(3,i)}_{\alpha\beta\gamma}] \\ & + 2[a^{(1,i)}_{\alpha} a^{(1,i)}_{\beta} a^{(2,i)}_{\gamma\delta} + a^{(1,i)}_{\alpha} a^{(1,i)}_{\gamma} a^{(2,i)}_{\beta\delta} + a^{(1,i)}_{\alpha} a^{(1,i)}_{\delta} a^{(2,i)}_{\beta\gamma} \\ & + a^{(1,i)}_{\beta} a^{(1,i)}_{\gamma} a^{(2,i)}_{\alpha\delta} + a^{(1,i)}_{\beta} a^{(1,i)}_{\delta} a^{(2,i)}_{\alpha\gamma} + a^{(1,i)}_{\gamma} a^{(1,i)}_{\delta} a^{(2,i)}_{\alpha\beta}] - 6a^{(1,i)}_{\alpha} a^{(1,i)}_{\beta} a^{(1,i)}_{\gamma} a^{(1,i)}_{\delta}\}, \end{aligned}$$

where the sum over i goes from 1 to N. Now since $\langle k_{\mu_1} \cdots k_{\mu_l} \rangle_i$ vanishes if there is an odd number of spatial indices, so does $A^{(l)}_{\mu_1 \ldots \mu_l}$. Consequently, if we use $(abcd)$ and $[abcd]$ to denote respectively $A^{(l)}_{\mu_1 \ldots \mu_l}$ and $a^{(l,i)}_{\mu_1 \ldots \mu_l}$, in which the indices $\mu_1 \cdots \mu_l$ take on the value 0 a times, the value 1 $2b$ times, the value 2 $2c$ times, and the value 3 $2d$ times (so that $l = a + 2b + 2c + 2d$), then we have

$$\begin{aligned} &(2000) = [2000] - [1000]^2, \\ &(0100) = [0100], \\ &(3000) = [3000] - 3[1000][2000] + 2[1000]^3, \\ &(1100) = [1100] - [1000][0100], \\ &(4000) = [4000] - 3[2000]^2 - 4[1000][3000] - 6[1000]^4 + 12[1000]^2[2000], \\ &(2100) = [2100] - [2000][0100] - 2[1000][1100] + 2[1000]^2[0100], \\ &(0200) = [0200] - 3[0100]^2, \\ &(0110) = [0110] - [0100][0010]. \end{aligned} \tag{A6}$$

The square brackets in (A6) actually depend on i. A sum of i from 1 to N of the right-hand side of (A6) is understood. For the 2D formulas, (A6) is still correct except that (0110) is irrelevant. For 4D cases, since $g_i(k)$ is spherically symmetrical, we may carry out the angular integrations in $[abcd]$ and arrive at the formula

$$[abcd] = \frac{(2b-1)!!\,(2c-1)!!\,(2d-1)!!}{[2(a+b+c+d)+1]!!} \langle a, b+c+d \rangle, \quad (-1)!! \equiv 1, \tag{A7}$$

with

$$\langle a, e \rangle \equiv 4\pi \int_0^\infty k^2 dk\, g_i(k) (k^0)^a (k^2)^e. \tag{A8}$$

We may now work out from Table I the contributions to Σ_c in (18) and (18′). We will first carry out the substitution for the 4D formulas. From (17) and (A5), we know that

$$\begin{aligned} &B^{00} \equiv B_T = (2000)^{-1}, \\ &B^{ij} \equiv B_S \delta_{ij} = (0100)^{-1} \delta_{ij}. \end{aligned} \tag{A9}$$

This leads to

$$(\det A^{(2)})^{-1/2} = B_S^{3/2} B_T^{1/2}. \tag{A10}$$

The various terms in Table I are

$$\begin{aligned} &Z_0 = \tfrac{1}{8}\{B_T^2(4000) + 6B_T B_S(2100) + 3B_S^2[(0200) + 2(0110)]\}, \\ &Z_1 = \tfrac{1}{12}\{B_T^3(3000)^2 + 9B_T B_S^2(1100)^2\}, \\ &Z_2 = \tfrac{1}{8}\{B_T^3(3000)^2 + 6B_T^2 B_S(3000)(1100) + 9(1100)^2 B_S^2 B_T\}, \\ &Z_3 = \tfrac{1}{2}\{B_T^2(3000) + 3B_T B_S(1100)\}, \\ &Z_4 = \tfrac{1}{2} B_T, \\ &Z_5 = \tfrac{1}{2} B_S. \end{aligned} \tag{A11}$$

In the case of the 2D formulas, (A6) is still valid, but instead of (A7) and (A8) we have

$$[ab00] \equiv \langle a, b \rangle = \int_{-\infty}^{\infty} g_i(k) (k^0)^a (k^2)^b dk. \tag{A12}$$

We still have

$$B^{00} \equiv B_T = (2000)^{-1}, \qquad B^{11} \equiv B_S = (0100)^{-1}, \tag{A13}$$

but now

$$(\det A^{(2)})^{-1/2} = (B_S B_T)^{1/2}, \tag{A14}$$

and the various terms in Table I become

$$\begin{aligned} Z_0 &= \tfrac{1}{8}\{B_T{}^2(4000) + 2B_T B_S(2100) + B_S{}^2(0200)\}, \\ Z_1 &= \tfrac{1}{12}\{B_T{}^3(3000)^2 + 3B_T B_S{}^2(1100)^2\}, \\ Z_2 &= \tfrac{1}{8}\{B_T{}^2(3000)^2 + 2B_T{}^2 B_S(3000)(1100) + B_T B_S{}^2(1100)^2\}, \\ Z_3 &= \tfrac{1}{2}\{B_T{}^2(3000) + B_T B_S(1100)\}, \\ Z_4 &= \tfrac{1}{2} B_T, \\ Z_5 &= \tfrac{1}{2} B_S . \end{aligned} \tag{A15}$$

Finally, we come to the special case when $g_i(k)$ is given by (A1) and (A2). Again we consider 4D cases first. Now (A8) can be evaluated explicitly. The result is

$$\langle 2k, n\rangle = \sum_{l=0}^{k} \binom{k}{l} (m_i^2)^l \langle 0, n+k-l\rangle , \tag{A16}$$

$$\langle 2k+1, n\rangle = \sum_{l=0}^{k} \binom{k}{l} (m_i^2)^l \langle 1, n+k-l\rangle , \tag{A17}$$

$$\langle 0, n\rangle = (2n+1)!!/(2\alpha_i)^n . \tag{A18}$$

Thus all the Z_i may be obtained from algebra, except possibly the computation of $\langle 1,0\rangle$ and $\langle 1,1\rangle$. If one prefers, even these two integrals can be reduced to modified Bessel functions:

$$\begin{aligned} \langle 1,0\rangle &= 4\pi \int_0^\infty \left(\frac{\alpha_i}{\pi}\right)^{3/2} \exp(-\alpha_i k^2)(k^2+m_i^2)^{1/2} k^2 dk \\ &= \left(\frac{\alpha_i}{\pi}\right)^{3/2} \left(\frac{\pi m_i^2}{\alpha_i}\right) \exp(\tfrac{1}{2}\alpha_i m_i^2) K_1(\tfrac{1}{2}\alpha_i m_i^2), \\ \langle 1,1\rangle &= 4\pi \int_0^\infty \left(\frac{\alpha_i}{\pi}\right)^{3/2} \exp(-\alpha_i k^2)(k^2+m_i^2)^{1/2} k^4 dk \\ &= \left(\frac{\alpha_i}{\pi}\right)^{3/2} \left(\frac{\pi m_i^4}{2\alpha_i}\right) \exp(\tfrac{1}{2}\alpha_i m_i^2)[K_2(\tfrac{1}{2}\alpha_i m_i^2) - K_1(\tfrac{1}{2}\alpha_i m_i^2)]. \end{aligned} \tag{A19}$$

For 2D cases, (A2) and (A12) are used. Equations (A16) and (A17) are still valid, but (A18) should be replaced by

$$\langle 0, n\rangle = (2n-1)!!/(2\alpha_i)^n , \qquad (-1)!! \equiv 1 . \tag{A20}$$

Moreover, $\langle 1,0\rangle$ and $\langle 1,1\rangle$ can also be evaluated. The result is

$$\begin{aligned} \langle 1,0\rangle &= \left(\frac{\alpha_i}{\pi}\right)^{1/2} \int_{-\infty}^{\infty} e^{-\alpha_i k^2} (k^2 + m_{i\perp}{}^2)^{1/2} dk \\ &= \left(\frac{\alpha_i}{\pi}\right)^{1/2} (\tfrac{1}{2} m_{i\perp}{}^2)\, e^{\alpha_i m_{i\perp}{}^2/2} [K_0(\tfrac{1}{2}\alpha_i m_{i\perp}{}^2) + K_1(\tfrac{1}{2}\alpha_i m_{i\perp}{}^2)], \\ \langle 1,1\rangle &= \left(\frac{\alpha_i}{\pi}\right)^{1/2} \int_{-\infty}^{\infty} e^{-\alpha_i k^2} (k^2 + m_{i\perp}{}^2)^{1/2} dk\; k^2 \\ &= \left(\frac{\alpha_i}{\pi}\right)^{1/2} (\tfrac{1}{2} m_{i\perp}{}^2) e^{\alpha_i m_{i\perp}{}^2/2} K_1(\tfrac{1}{2}\alpha_i m_i^2)/\alpha . \end{aligned} \tag{A21}$$

Finally, let us remark that both for the 4D and the 2D, we can see from (A6)–(A8), (A16)–(A18), and (A20) that

$$(0200) = (0110) = 0 . \tag{A22}$$

---

*On sabbatical leave from Department of Physics, McGill University. Research partly supported by the National Research Council of Canada.

[1]R. C. Hwa, Phys. Rev. Letters 26, 1143 (1971).

[2]R. C. Hwa and C. S. Lam, Phys. Rev. Letters 27, 1098 (1971).

[3]M. Jacob and R. Slansky, Phys. Letters 37B, 408 (1971).

[4]R. K. Adair, Phys. Rev. D 5, 1105 (1972).

[5]R. C. Hwa and C. S. Lam, Phys. Rev. D 5, 766 (1972); M. Jacob, R. Slansky, and C. C. Wu, Phys. Letters 38B, 85 (1972).

[6]R. C. Hwa, Phys. Rev. Letters 28, 1487 (1972).

[7]E. L. Berger and M. Jacob, Phys. Rev. D 6, 1930 (1972); E. L. Berger, B. Y. Oh, and G. A. Smith, Phys. Rev. Letters 28, 322 (1972).

[8]The only exception is Ref. 4, where the conservation law is taken into account numerically via the Monte Carlo method. Although this is one way of doing it, a heavy reliance on numerical methods tends to obscure what physical effects this conservation law would produce. To gain an understanding of what is involved, this must be supplemented by a theoretical analysis, clearly displaying various effects before numbers are put in.

[9]E. M. Gordon and C. S. Lam, Lett. Nuovo Cimento 4, 749 (1972).

[10]A. Bialas *et al.*, Phys. Letters 39B, 211 (1972).

[11]F. Lurçat and P. Mazur, Nuovo Cimento 31, 140 (1964); E. H. de Groot and Th. W. Ruijgrok, Nucl. Phys. B27, 45 (1971); E. H. de Groot, thesis (unpublished); Y.-A. Chao, Nucl. Phys. B40, 475 (1972); L. Y. Chang, Phys. Rev. D 4, 2137 (1971).

[12]A. I. Khinchin, *Mathematical Foundations of Statistical Mechanics* (Dover, New York, 1949).

[13]See, e.g., C. S. Lam, Nuovo Cimento 38, 1755 (1965).

[14]J. Benecke, T. T. Chou, C. N. Yang, and E. Yen, Phys. Rev. 188, 2159 (1969); T. T. Chou and C. N. Yang, Phys. Rev. Letters 25, 1072 (1970).